Journal of Computational Acoustics,

FICTITIOUS DOMAINS, MIXED FINITE ELEMENTS AND PERFECTLY MATCHED LAYERS FOR 2D ELASTIC WAVE PROPAGATION

E. BÉCACHE, P. JOLY and C. TSOGKA
INRIA, Domaine de Voluceau-Rocquencourt, BP 105, F-78153 Le Chesnay Cédex
eliane.becache@inria.fr, patrick.joly@inria.fr and chrysoula.tsogka@inria.fr

Received (to be inserted
Revised by Publisher)

We design a new and efficient numerical method for the modelization of elastic wave propagation in domains with complex topographies. The main characteristic is the use of the fictitious domain method for taking into account the boundary condition on the topography: the elastodynamic problem is extended in a domain with simple geometry, which permits us to use a regular mesh. The free boundary condition is enforced introducing a Lagrange multiplier, defined on the boundary and discretized with a non-uniform boundary mesh. This leads us to consider the first order velocity-stress formulation of the equations and particular mixed finite elements. These elements have three main non-standard properties: they take into account the symmetry of the stress tensor, they are compatible with mass lumping techniques and lead to explicit time discretization schemes, and they can be coupled with the Perfectly Matched Layer technique for the modeling of unbounded domains. Our method permits us to model wave propagation in complex media such as anisotropic, heterogeneous media with complex topographies, as it will be illustrated by several numerical experiments.

1. Introduction

In this work, we present a fictitious domain method for modeling time dependent elastic wave propagation in complex media such as heterogeneous anisotropic media of complex geometries. From an industrial point of view, the main applications concerned by this work are the study of seismic waves in media with complex topographies and the non-destructive testing (diffraction by a crack of complex geometry). In this paper we will restrict ourselves in the first application considering the elastodynamic problem in a domain with a complex topography (see Fig. 1).

Among the possible methods for solving this problem, the finite difference method is one of the most attractive. It uses a regular mesh with an explicit time discretization, and therefore is very efficient from the computational point of view. Its main drawback is that it produces spurious diffractions when the boundary does not fit the grid mesh (see Fig. 1-left). An alternative is to use finite elements with a non-uniform mesh, that can fit exactly

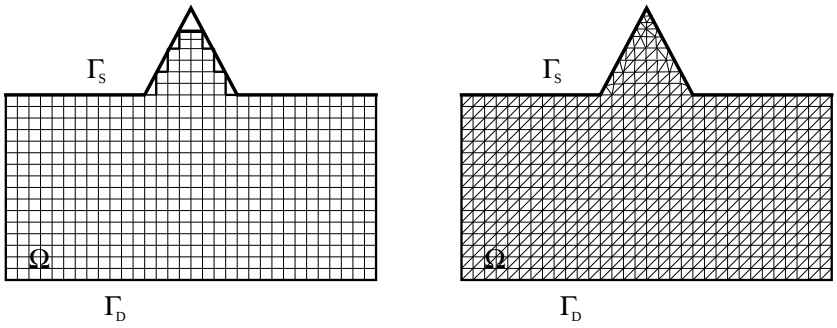

Figure 1: Left: finite difference method (staircase approximation). Right: Finite elements

the complex geometry of the boundary, see Fig. 1-right. Nevertheless, other disadvantages are introduced. The numerical implementation is much more difficult, the efficiency may be decreased by the unstructured nature of the data, and finally the CFL stability is affected: in order to fit the complex geometry of the boundary, the mesh may contain elements of very small size, which implies, because of the CFL stability condition, the use of a very small time step if one uses an explicit scheme.

In this work we propose the use of an alternative method, the fictitious domain method (also called the domain embedding method) which combines the efficiency of the finite difference method (regular meshes and explicit time discretization schemes) with a good approximation of the topography. This method was initially developed for solving problems with complex geometries[2,17], particularly in the stationary case. The study of the fictitious domain method for time dependent problems has started a few years ago[18,12,15]. Its principle is to extend the solution to a simple shape domain independent of the boundary of complex geometry (typically a rectangle in 2D), containing the domain of interest, and to impose the boundary condition via the introduction of a Lagrange multiplier on the boundary. The main point is that we have now two unknowns, the extended function, defined in the enlarged simple shape domain and the auxiliary variable, defined on the boundary of complex geometry, so that the mesh for computing the extended function can be chosen independently of the geometry of the boundary. In particular, the use of regular grids allows simple and efficient computations. Of course, we have to pay for this advantage in terms of some additional computational cost due to the introduction of the new boundary unknown. However, the final numerical scheme appears to be a slight perturbation of the scheme for the problem without obstacle so that this cost may be considered as marginal.

In the problem we are interested in, the boundary condition is a free surface condition, that is, the normal stress is zero on the surface: in order to consider this condition as an equality constraint, we are led in a natural way to use the mixed velocity-stress formulation for elastodynamics. Then the Lagrange multiplier can be interpreted as the jump of the velocity through the surface. Another advantage of working with the first-order mixed velocity-stress formulation is that it is well suited to the use of a new absorbing layer model for bounding the computational domain: the Perfectly Matched Layers (PML), introduced

by Berenger[10] for the 2D Maxwell problem and that can be extended to elastodynamics. This model has astonishing properties: the reflection coefficient at the interface between the layer and the free medium is zero for all frequencies and angles of incidence. The extension of this model to elastodynamics is natural when using the mixed velocity-stress formulation.

These considerations lead us to find an efficient approximation of the time domain mixed velocity-stress formulation. In particular for stability reasons (conservation of energy), we have decided to use a discretization procedure in space based on a variational formulation of the velocity stress system, which is a first order hyperbolic system. At this stage, our main requirement is to define a spatial discretization which allows us to obtain an explicit time discretization scheme (mass-lumping).

Several mixed finite element methods are proposed in the literature especially for plane elasticity. We refer for example to PEERS element introduced by D. N. Arnold, F. Brezzi and J. Douglas[1] and more recently to the work of R. Stenberg[22] and M. Morley[20]. One of the well known difficulties for mixed elements in elasticity is to take into account the symmetry of the stress tensor. The method used in these papers [1,22,20] consists in working with a space of non-necessarily symmetric tensors and imposing the symmetry in a weak way via the introduction of a Lagrange multiplier. Although these methods are very interesting for plane elasticity, we did not retain them as they lead to an implicit scheme in time.

That is why we have constructed an original mixed finite element (inspired from the second Nédélec's family[21]) using spaces of symmetric tensors for the stress[6]. These spaces will fit our objectives. The error analysis of these mixed finite elements will not be discussed here, we refer the reader to[7,8], where a non-classical convergence theory is presented.

The present paper is organized as follows. In §2 we briefly recall the equations of elastodynamics. In §3 we describe the fictitious domain method applied to elastodynamics, with a free surface boundary condition. We explain in §4 how to apply the PML to the elastodynamic problem. We introduce in §5.2 the new family of mixed finite elements for linear elasticity, which permits us to make mass lumping. The dispersion and stability analysis of the lowest order element is presented in §6 in the case of an homogeneous isotropic medium. Finally, we show in §7 some numerical results.

2. The linear elastodynamic problem

We want to solve the linear elastodynamic problem with a complex topography (see Fig. 2-left). The solution is governed by the elastic wave equation in Ω and we impose the free surface condition on Γ_S. For the sake of simplicity a Dirichlet condition is assumed on the exterior boundary Γ_D but we will see in §4 how we can take into account the modelization of an unbounded domain by an efficient absorbing layer model (PML).

Notations. We identify the space of 2×2 tensors with the space $\mathcal{L}(\mathbb{R}^2)$ of linear applications from $\mathbb{R}^2$ to $\mathbb{R}^2$. We define the linear form, $\mathbf{as}(\sigma) = \sigma_{12} - \sigma_{21}$, and the subspace of

symmetric tensors of $\mathcal{L}(\mathbb{R}^2)$:

$$\mathcal{L}^s(\mathbb{R}^2) = \left\{ \sigma \in \mathcal{L}(\mathbb{R}^2) \ / \ \mathbf{as}(\sigma) = 0 \right\}.$$

The scalar product in $\mathcal{L}(\mathbb{R}^2)$ is defined by $\sigma : \tau = \sigma_{ij}\tau_{ij}$, for all (σ, τ) in $\mathcal{L}(\mathbb{R}^2)$ and $|\sigma|$ is the associated norm. Finally, the divergence of a tensor is defined as:

$$\text{div } \sigma = \begin{bmatrix} \dfrac{\partial \sigma_{11}}{\partial x_1} + \dfrac{\partial \sigma_{12}}{\partial x_2} \\ \dfrac{\partial \sigma_{21}}{\partial x_1} + \dfrac{\partial \sigma_{22}}{\partial x_2} \end{bmatrix}.$$

The continuous displacement problem. We want to solve the elastodynamic problem:

$$\begin{cases} \varrho \dfrac{\partial^2 u}{\partial t^2} - \text{div } \sigma(u) = g & \text{in } \Omega, \\ u = 0 & \text{on } \Gamma_D, \\ \sigma \cdot n = 0 & \text{on } \Gamma_S, \end{cases} \tag{2.1}$$

with some initial conditions at time $t = 0$ that we will systematically omit in the following. In (2.1), $u = (u_1, u_2)^t$ denotes the displacement, $\sigma(u)$ is the stress tensor, $\varrho = \varrho(x)$ is the density and $x = (x_1, x_2)$. Consider $\varepsilon(u)$ the strain tensor, i.e.,

$$\varepsilon_{ij}(u) = \frac{1}{2}\left(\frac{\partial u_i}{\partial x_j} + \frac{\partial u_j}{\partial x_i} \right).$$

The stress tensor is related to the strain tensor by Hooke's law

$$\sigma(u)(x,t) = C(x)\varepsilon(u)(x,t),$$

where $C(x)$ is a 4×4 positive tensor having the classical properties of symmetry[3]. The density is assumed to be bounded,

$$0 < \varrho_- \leq \varrho(x) \leq \varrho_+ < +\infty \quad \text{p.p. } x \in \Omega,$$

We set $A(x) = C(x)^{-1}$ and we suppose that $A(x)$ satisfies :

$$\forall \sigma \in \mathcal{L}^s(\mathbb{R}^2) \quad 0 < \alpha \left|\sigma\right|^2 \leq A(x)\sigma : \sigma \leq M \left|\sigma\right|^2.$$

In the following, we assume that Γ_S is a piecewise C^1 Lipschitz curve which permits us to define the Sobolev spaces $H^s(\Gamma_S)$ for any $s < 3/2$ (see [19]).

3. The Fictitious domain method for the elastodynamic problem

In this section we apply the fictitious domain method for solving the elastodynamic problem (2.1). As explained in the introduction, this method consists in extending the

solution of problem (2.1) to a larger domain of simple geometry (see Fig. 2) and in taking into account the boundary condition in a weak way, thanks to the introduction of a Lagrange multiplier. To do so with the free surface condition (Neumann condition), σ has necessarily to be one of the unknowns. Therefore, we have to write the elastodynamic problem (2.1) as a first order hyperbolic system, the so called velocity-stress system.

Remark 1 *More generally, the fictitious domain method can be used for the essential conditions, i.e., conditions that can be taken into account in the functional space.*

3.3.1. *The mixed velocity-stress formulation*

Problem (2.1) is equivalent to the mixed velocity-stress system :

$$\left\{\begin{array}{lcll} \varrho\dfrac{\partial v}{\partial t} - \text{div } \sigma &=& f \quad \text{in } \Omega & (i) \\ A\dfrac{\partial \sigma}{\partial t} - \varepsilon(v) &=& 0 \quad \text{in } \Omega & (ii) \\ v &=& 0 \quad \text{on } \Gamma_D & (iii) \\ \sigma \cdot n &=& 0 \quad \text{on } \Gamma_S & (iv) \end{array}\right. , \tag{3.2}$$

where $v = \dfrac{\partial u}{\partial t}$ is the velocity in Ω and $f = \dfrac{\partial g}{\partial t}$. Considering the spaces

$$\left\{\begin{array}{l} X = \left\{\tau \in (H(\text{div },\Omega))^2, \quad \tau \cdot \vec{n} = 0 \text{ on } \Gamma_S\right\}, \\ X^s = \left\{\tau \in X, \quad \tau \text{ symmetric}\right\}, \\ M = (L^2(\Omega))^2, \end{array}\right.$$

the variational formulation of problem (3.2) is :

$$\left\{\begin{array}{ll} \text{Find } (\sigma, v) \in X^s \times M \text{ such that:} & \\ \dfrac{d}{dt}a(\sigma,\tau) + b(\tau, v) = 0, & \forall \tau \in X^s, \\ \dfrac{d}{dt}c(v,w) - b(\sigma, w) = (f, w), & \forall w \in M, \end{array}\right. \tag{3.3}$$

where we have set :

$$\left\{\begin{array}{ll} a(\sigma,\tau) = \displaystyle\int_\Omega A\sigma : \tau dx, & \forall (\sigma,\tau) \in X^s \times X^s, \\ c(v,w) = \displaystyle\int_\Omega \varrho v \cdot w dx, & \forall (v,w) \in M \times M, \\ b(\tau,w) = \displaystyle\int_\Omega \text{div } \tau \cdot w dx, & \forall (\tau,w) \in X^s \times M. \end{array}\right. \tag{3.4}$$

This system satisfies the classical energy estimate $\mathbf{E}(t) = \mathbf{E}(0) + \int_0^t (f(s), v(s))_M ds$, the energy being defined as

$$\mathbf{E}(t) = \frac{1}{2}(A\sigma, \sigma)_H + \frac{1}{2}(\rho v, v)_M \equiv \frac{1}{2}a(\sigma, \sigma) + \frac{1}{2}c(v, v).$$

Remark 2 *To obtain this formulation it is crucial to work in the space X^s of symmetric tensors : only in this space operators $-\varepsilon$ and* div *are adjoint.*

3.3.2. *Application of the fictitious domain method to elastodynamics*

We now extend solution of problem (3.2) to the solution, still denoted (v, σ) for simplicity, of a problem posed in an enlarged domain C, which is a simple rectangle (see Fig. 2), with Dirichlet conditions on the external boundary,

$$\left\{ \begin{array}{lcll} \varrho \dfrac{\partial v}{\partial t} - \text{div } \sigma & = & f & \text{in } C \\ A\dfrac{\partial \sigma}{\partial t} - \varepsilon(v) & = & \Lambda \delta_{\Gamma_S} & \text{in } C \\ v & = & 0 & \text{on } \partial C \\ \sigma \cdot n & = & 0 & \text{on } \Gamma_S \end{array} \right. , \tag{3.5}$$

where Λ is the tensor of components $\Lambda_{ij} = \lambda_i n_j$, λ being a new unknown, defined only on the boundary Γ_S. We introduce the spaces (denoted also X, X^s and M for simplicity)

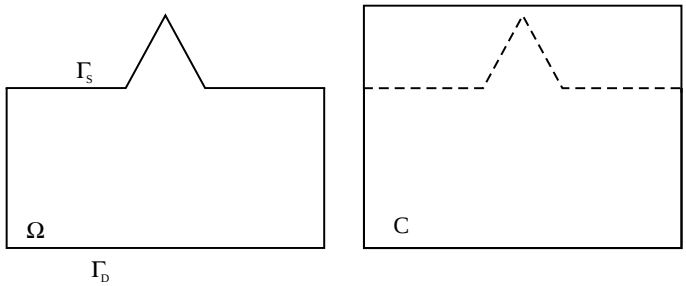

Figure 2: Left: the original domain. Right: the enlarged domain

$$\left\{ \begin{array}{l} X = \{\tau \in (H(\text{div }, C))^2\} \ ; \ X^s = \{\tau \in X, \tau \text{ symmetric }\}, \\ M = (L^2(C))^2 \ ; \ \mathcal{G} = (H^{1/2}(\Gamma_S))^2, \end{array} \right. \tag{3.6}$$

defined on the whole rectangle C. The variational formulation of (3.5) can be written

as follows:

$$\left\{\begin{array}{ll} \text{Find } (\sigma, v, \lambda) \in X^s \times M \times \mathcal{G} \text{ such that:} & \\ \\ \dfrac{d}{dt}a(\sigma,\tau) + b(\tau, v) - s(\tau,\lambda) = 0, & \forall \tau \in X^s \quad (i) \\ \\ \dfrac{d}{dt}c(v,w) - b(\sigma, w) = (f, w), & \forall w \in M \quad (ii) \\ \\ s(\sigma,\mu) = 0, & \forall \mu \in \mathcal{G} \quad (iii) \end{array}\right. \tag{3.7}$$

the bilinear forms $a(\cdot,\cdot), b(\cdot,\cdot), c(\cdot,\cdot)$ being defined by (3.4) (with C instead of Ω), with

$$s(\tau,\lambda) = \langle \tau\vec{n}, \lambda\rangle_{\Gamma_S} \qquad \forall (\tau,\lambda) \in X^s \times \mathcal{G}.$$

Actually the unknown λ can be interpreted as a Lagrange multiplier corresponding to $[v]_{\Gamma_S}$. Obviously, the restriction of (v,σ) to Ω still satisfies (3.2). Moreover, we can remark that the restriction of the solution to $\overline{\Omega}^c$ (where $\overline{\Omega}^c$ denotes the complementary of $\overline{\Omega}$ in C) also satisfies (3.2) where Ω is replaced by $\overline{\Omega}^c$ (and Γ_D denotes $\partial C \cap \partial\overline{\Omega}^c$). Now if we multiply (3.2)-(ii) with a function $\tau \in X^s$ (X^s being defined by (3.6)), and integrate in $\Omega \cup \overline{\Omega}^c$, an integration by parts of the second term gives

$$-\int_{\Omega\cup\Omega^c} \varepsilon(v)\tau dx = \int_{\Omega\cup\Omega^c} v.\mathrm{div}\tau dx - \langle \tau\vec{n}, v^+ - v^-\rangle_{\Gamma_S} \equiv b(\tau, v) - s(\tau, [v]_{\Gamma_S}),$$

which yields (3.7-(i)), if we set $\lambda = [v]_{\Gamma_S}$. Since the free surface boundary condition on Γ_S is not taken into account anymore in the new definition of space X, it has to be imposed in the formulation, this is done with (3.7-(iii)).

Remark 3 *There is a strong link between the fictitious domain method and the boundary integral equation method. The extended solution is chosen such that the normal stress is continuous through Γ_S and the new unknown corresponds to the unknown of the BIE obtained using a double layer potential representation for v (see[5]).*

3.3.3. *Semi-discretization in space*

Consider now finite dimension spaces $X_h^s \subset X^s$, $M_h \subset M$ and $\mathcal{G}_H \subset \mathcal{G}$ with classical approximation properties, which will be specified in §5 for our particular choice of approximation spaces. The semi-discretization in space of problem (3.7) can be written:

$$\left\{\begin{array}{ll} \text{Find } (\sigma_h, v_h, \lambda_H) \in X_h^s \times M_h \times \mathcal{G}_H \text{ such that :} & \\ \\ \dfrac{d}{dt}a(\sigma_h,\tau_h) + b(\tau_h, v_h) - s(\tau_h,\lambda_H) = 0, & \forall \tau \in X_h^s, \\ \\ \dfrac{d}{dt}(v_h, w_h) - b(\sigma_h, w_h) = (f, w_h), & \forall w_h \in M_h, \\ \\ \langle \sigma_h\vec{n}, \mu_H\rangle_{\Gamma_S} = 0, & \forall \mu_H \in \mathcal{G}_H. \end{array}\right. \tag{3.8}$$

We introduce here $B_{N_1} = \{\tau_i\}_{i=1}^{N_1}$, $B_{N_2} = \{w_i\}_{i=1}^{N_2}$ and $B_{N_3} = \{\mu_i\}_{i=1}^{N_3}$ the bases of X_h^s, M_h and $\mathcal{G}_H$ respectively ($N_1 = \dim X_h^s$, $N_2 = \dim M_h$ and $N_3 = \dim \mathcal{G}_H$), $[\Sigma_h] = (\Sigma_1, ..., \Sigma_{N_1})$, $[V_h] = (V_1, ..., V_{N_2})$ and $[\lambda_H] = (\Lambda_1, ..., \Lambda_{N_3})$ the coordinates of σ_h, v_h and λ_H in the bases B_{N_1}, B_{N_2} and B_{N_3}. In these bases, (3.8) can be written in the following matrix form:

$$\left\{\begin{array}{l} \text{Find } (\Sigma_h, V_h, \lambda_H) \in L^2(0,T;\mathbb{R}^{N_1}) \times L^2(0,T;\mathbb{R}^{N_2}) \times L^2(0,T;\mathbb{R}^{N_3}) \text{ such that:} \\ \\ \dfrac{d}{dt} A_h \Sigma_h + B_h^\star V_h - S_h \lambda_H = 0, \\ \\ C_h \dfrac{dV_h}{dt} - B_h \Sigma_h = F_h, \\ \\ S_h^\star \Sigma_h = 0, \end{array}\right. \tag{3.9}$$

where $M^\star$ denotes the transpose of the matrix M. In practice, and this is the interesting point in the fictitious domain method, we introduce two meshes: the volume unknowns (V_h, Σ_h) are defined on a regular grid, $\mathcal{T}_h$ made of squares of size h while the surface unknown λ_H is computed on a non-uniform mesh on Γ_S, $\mathcal{T}_H$ made of segments of size H_j, $H = \sup_j H_j$, see Fig. 8-left. From the theoretical point of view, the well-posedness of (3.9) and the convergence of the method is linked to the verification of a uniform inf-sup condition which leads to a compatibility condition between the boundary mesh and the uniform mesh[16] of the form $H \geq Ch$ ($C \simeq 1.3$ for our choice of approximation spaces (5.23),(5.24)).

At this point we can see the importance of mass-lumping: assume for the moment that we can find appropriate finite element spaces and the adequate quadrature formulas in order to achieve mass-lumping on the matrix A_h, we can then eliminate the unknown Σ_h (which implies important savings in memory requests especially in the 3D case) and write system (3.9) as the second order system in time :

$$\left\{\begin{array}{ll} \text{Find } (V_h, \lambda_H) \in L^2(0,T;\mathbb{R}^{N_2}) \times L^2(0,T;\mathbb{R}^{N_3}) & \text{such that:} \\ \\ C_h \dfrac{d^2 V_h}{dt^2} + B_h A_h^{-1} B_h^\star V_h - B_h A_h^{-1} S_h \lambda_H = \dfrac{dF_h}{dt}, & \\ \\ -S_h^\star A_h^{-1} B_h^\star V_h + S_h^\star A_h^{-1} S_h \lambda_H = 0. & \end{array}\right. \tag{3.10}$$

We describe in §5.2 an appropriate choice for X_h^s, M_h (the lowest-order element of a new family of mixed finite elements[6,7]) which allows us to obtain mass-lumping for A_h.

3.3.4. *Total discretization*

For the time discretization of problem (3.10) we restrict ourselves to the classical second

order centered finite differences approximation :

$$\left\{\begin{array}{l} \text{Find } (V_h^{n+1}, \lambda_H^n) \in \mathbb{R}^{N_2} \times \mathbb{R}^{N_3} \text{ such that :} \\ \\ C_h \dfrac{V_h^{n+1} - 2V_h^n + V_h^{n-1}}{\Delta t^2} + B_h A_h^{-1} B_h^\star V_h^n - B_h A_h^{-1} S_h \lambda_H^n = \dfrac{F_h^{n+1/2} - F_h^{n-1/2}}{\Delta t} \quad (i) \\ \\ S_h^\star A_h^{-1} S_h \lambda_H^n = S_h^\star A_h^{-1} B_h^\star V_h^n \quad (ii) \end{array}\right. \tag{3.11}$$

This is an explicit scheme only if C_h is also a diagonal matrix, which, in practice, is not difficult to achieve. This comes from the fact that $M_h \subset L^2$ and thus can be constructed with discontinuous functions and, from now on, we assume that C_h is diagonal . The additional terms, coming from the coupling with the fictitious domain method are the terms containing the unknown λ_H^n. This means that, without topography, we would have to solve

$$\frac{V_h^{n+1} - 2V_h^n + V_h^{n-1}}{\Delta t^2} + C_h^{-1} B_h A_h^{-1} B_h^\star V_h^n = C_h^{-1} \frac{F_h^{n+1/2} - F_h^{n-1/2}}{\Delta t} \tag{3.12}$$

which can be reinterpreted as a finite difference scheme (see §6) and is comparable from the computational point of view to the classical finite difference scheme. Therefore, the additional cost for taking into account the topography thanks to the fictitious domain method, compared to the classical finite difference scheme, is due to the system (3.11)-(ii). The matrix of this system is of small size (number of degrees of freedom on Γ_S) and independent of the step n, so that it can be factorized once and we only have to perform a forward backward solve at each time step. Note that the term λ_H^n in equation (3.11)-(i) can be interpreted as an additional source term located on the boundary.

Remark 4 • *System (3.10) has the advantage of being a second-order system in time : it is easier to get higher-order discretization in time, using the modified equation technique (see*[14]*), than for the first-order system.*
• *The invertibility of the matrix $S_h^\star A_h^{-1} S_h$ of System (3.11)-(ii) (and thus the well posedness of ((3.11)) is assured by the inf-sup condition already mentioned before (needed for the convergence of the method).*

An important point is that the CFL stability condition for (3.11) is the same as for (3.12), i.e., for the discretized problem posed in the whole rectangle C without topography, which means that the use of the fictitious domain method does not affect the stability condition. Actually, assume that there is no source term (i.e., $F = 0$), then we can prove that, for the solution of (3.11), the following quantity is conserved

$$E^{n+1/2} = (C_h \frac{V_h^{n+1} - V_h^n}{\Delta t}, \frac{V_h^{n+1} - V_h^n}{\Delta t}) + (B_h A_h^{-1} B_h^\star V_h^{n+1}, V_h^n),$$

which is exactly the discrete energy of (3.12) (see[12] for more details).

We will see in §6.2 what is the stability condition for our particular choice of spaces X_h^s and M_h, in a case of a homogeneous, isotropic elastic medium.

4. A new absorbing layer model (P.M.L)

A new absorbing layer model, the Perfectly Matched Layer model was introduced by Berenger[10] for the 2D Maxwell problem. This model has astonishing properties: the reflection coefficient at the interface between the layer and the free medium is zero for all frequencies and angles of incidence. This model can be extended to general first order hyperbolic systems, and in particular to the first order velocity-stress formulation (see[13] for more details). In this section, we explain the basic principles of this model in the general case of a first order hyperbolic system and then we extend this model to elastodynamics.

4.4.1. *The PML model for a general first order hyperbolic system*

Consider the following first order hyperbolic system, posed initially in the space $\mathbb{R}^2$:

$$\begin{cases} \dfrac{\partial u}{\partial t} = A\dfrac{\partial u}{\partial x_1} + B\dfrac{\partial u}{\partial x_2}, \qquad u \in \mathbb{R}^m & (a) \\ u(x_1, x_2, 0) = u^0(x_1, x_2) & (b) \end{cases} \tag{4.13}$$

Suppose that the support of initial data u^0 is in the left half-space, we would like to substitute problem (4.13) by an equivalent one posed in the left half-space. The basic principle of the PML model is to couple the equation in the left half-space with an equation in the right half-space such that there is *no reflection* at the interface and that the wave *decreases exponentially* inside the layer. We first introduce the following system

$$\begin{cases} u = u^{\parallel} + u^{\perp}, \\ \dfrac{\partial u^{\parallel}}{\partial t} = B\dfrac{\partial u}{\partial x_2}, \\ \dfrac{\partial u^{\perp}}{\partial t} = A\dfrac{\partial u}{\partial x_1}, \end{cases} \tag{4.14}$$

where the index $\parallel$ (resp. $\perp$) means that we keep only the derivatives parallel to the interface, i.e., the x_2-derivatives (resp. orthogonal, i.e., the x_1-derivatives). It is easy to see that system (4.14) implies (4.13)-(a).

Secondly we define a new wave, v, solution of (4.14) in the left half-space and satisfying a new system in the right half-space, involving a damping on the normal component :

$$\begin{cases} v = v^{\parallel} + v^{\perp}, \\ \dfrac{\partial v^{\parallel}}{\partial t} = B\dfrac{\partial v}{\partial x_2}, \\ \dfrac{\partial v^{\perp}}{\partial t} + d(x_1)v^{\perp} = A\dfrac{\partial v}{\partial x_1}, \end{cases} \tag{4.15}$$

where the damping parameter $d(x_1)$ is positive and satisfies : $d(x_1) = 0, \quad \forall x_1 \leq 0$.

Now, consider a plane wave u, solution of (4.13)-(a), i.e., of the form :

$$u(x_1, x_2, t) = u_0 \, e^{-i(k_1 x_1 + k_2 x_2 - \omega t)}, \tag{4.16}$$

where u_0 satisfies the dispersion relation :

$$u_0 + \frac{k_1}{\omega} A u_0 + \frac{k_2}{\omega} B u_0 = 0. \tag{4.17}$$

We have the following theorem :

Theorem 1 *There exists a unique plane wave, v, solution of system (4.15) of the form*

$$v(x_1, x_2, t) = u_0 \, e^{-i(k_1 x_1 + k_2 x_2 - \omega t)} e^{\alpha(x_1)}, \tag{4.18}$$

satisfying :

- *$v \equiv u$ in the left half-space $x_1 \leq 0$ (no reflection)*
- *v is damped in the right half-space*
- *the damping coefficient in the absorbing layer is*

$$\frac{|\, v(x_1, x_2, t) \,|}{|\, u(x_1, x_2, t) \,|} = e^{\alpha(x_1)} = \exp\left(-\frac{k_1}{\omega} \int_0^{x_1} d(\xi) d\xi \right), \quad x_1 > 0.$$

Proof: See[13] ■

Remark 5 *Note that the damping is exponentially decreasing, depending on the direction of propagation of the wave: it decreases very fast for a wave propagating normally to the interface and more and more slowly as the direction approaches the parallel to the interface.*

In practice, we introduce a boundary, with a Dirichlet condition at $x_1 = \delta$, to bound the layer, and we solve (4.13)-(a) in the left half-space and (4.15) in the right half-space. This

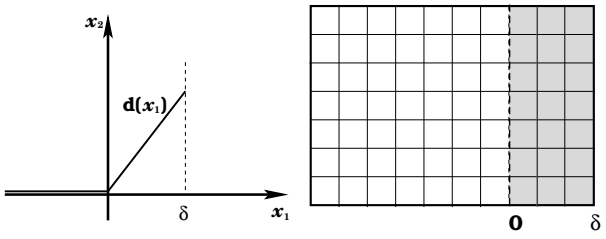

Figure 3: The damping parameter

new boundary produces a reflection, but, since the wave decreases exponentially in the layer, the reflection coefficient becomes quickly very small. This coefficient depends on the choice of $d(x_1)$ and on the size δ of the layer. One has interest to choose a layer large enough in

order to get a small reflection coefficient, but not too large in order to avoid increasing the additional computational cost too much.

4.4.2. *Application to elastodynamics*

Now consider the 2D elastodynamic problem written as a first order hyperbolic system, the velocity-stress system :

$$\left\{ \begin{array}{rcl} \varrho \dfrac{\partial v}{\partial t} - \text{div } \sigma & = & 0 \quad \text{in } \Omega, \\ A \dfrac{\partial \sigma}{\partial t} - \varepsilon(v) & = & 0 \quad \text{in } \Omega. \end{array} \right. \tag{4.19}$$

We use the usual identification of tensor σ with the vector (still denoted by σ) defined as

$$\sigma_1 = \sigma_{11} \ ; \ \sigma_2 = \sigma_{22} \ ; \ \sigma_3 = \sigma_{12}.$$

We can write (4.19) in the following matrix form :

$$\left\{ \begin{array}{l} \varrho \dfrac{\partial v}{\partial t} = D^{\perp} \dfrac{\partial \sigma}{\partial x_1} + D^{\parallel} \dfrac{\partial \sigma}{\partial x_2} \quad \text{in } \Omega, \\ A \dfrac{\partial \sigma}{\partial t} = E^{\perp} \dfrac{\partial v}{\partial x_1} + E^{\parallel} \dfrac{\partial v}{\partial x_2} \quad \text{in } \Omega, \end{array} \right. \tag{4.20}$$

with

$$D^{\parallel} = \begin{bmatrix} 0 & 0 & 1 \\ 0 & 1 & 0 \end{bmatrix} \ ; \ D^{\perp} = \begin{bmatrix} 1 & 0 & 0 \\ 0 & 0 & 1 \end{bmatrix} \ ; \ E^{\parallel} = \begin{bmatrix} 0 & 0 \\ 0 & 1 \\ 1 & 0 \end{bmatrix} \ ; \ E^{\perp} = \begin{bmatrix} 1 & 0 \\ 0 & 0 \\ 0 & 1 \end{bmatrix}. \tag{4.21}$$

Applying the previous result, we get the following system in the Perfectly Matched Layer

$$\left\{ \begin{array}{ll} v = v^{\parallel} + v^{\perp}, & \sigma = \sigma^{\parallel} + \sigma^{\perp}, \\ \varrho \dfrac{\partial v^{\parallel}}{\partial t} = D^{\parallel} \dfrac{\partial \sigma}{\partial x_2}, & \varrho \dfrac{\partial v^{\perp}}{\partial t} + d(x_1) v^{\perp} = D^{\perp} \dfrac{\partial \sigma}{\partial x_1}, \\ A \dfrac{\partial \sigma^{\parallel}}{\partial t} = E^{\parallel} \dfrac{\partial v}{\partial x_2}, & A \dfrac{\partial \sigma^{\perp}}{\partial t} + d(x_1) A \sigma^{\perp} = E^{\perp} \dfrac{\partial v}{\partial x_1}. \end{array} \right. \tag{4.22}$$

5. Choice of the approximation spaces

5.5.1. *Approximation space for the Lagrange multiplier, $\mathcal{G}_H$*

We denote by $\mathcal{T}_H$ a triangulation of Γ_S made of segments S_j of size H_j, and $H = \sup_j H_j$. In practice, we use for $\mathcal{G}_H$ the space of piecewise continuous linear functions:

$$\mathcal{G}_H = \left\{ \mu_H \in (C^0(\Gamma_S))^2, / \forall S_j \in \mathcal{T}_H, \ \mu_H \Big|_{S_j} \in (P_1(S_j))^2 \right\}, \tag{5.23}$$

which is the classical approximation of $H^{1/2}(\Gamma_S)$ and satisfies the approximation properties:

$$\begin{cases} \forall \lambda \in \mathcal{G},\ \lim\limits_{H\to 0} \inf\limits_{\mu_H \in \mathcal{G}_H} \|\lambda - \mu_H\|_{\mathcal{G}} = 0, \\ \forall \lambda \in H^{3/2-\varepsilon}(\Gamma_S)\ (\varepsilon > 0),\ \inf\limits_{\mu_H \in \mathcal{G}_H} \|\lambda - \mu_H\|_{\mathcal{G}} \leq C H^{3/2-\varepsilon} \|\lambda\|_{3/2-\varepsilon}\,. \end{cases}$$

5.5.2. *Approximation spaces for* (σ, v)*: construction of the* $Q_1^{\rm div} - Q_0$ *mixed finite element*

As explained previously (see §3.2), in order to achieve mass lumping on matrix A_h we have to find appropriate finite element spaces. As this is independent of the presence or not of the boundary Γ_S, we consider the problem without "obstacle", i.e., problem (3.4), and we assume that Ω is the square $]0,1[\times]0,1[$. We denote by $\mathcal{T}_h$ a regular mesh of Ω composed by squares (K) of side $h = 1/N$. Our aim is to use a space discretization method that can lead after time discretization to an explicit scheme. To do so, we are led to construct a new finite element method which fits our aim. For simplicity we present the lowest order element, so-called $Q_1^{\rm div} - Q_0$ element, but this construction can be easily generalized to higher orders and to the 3D problem[8,7]. We consider the approximate spaces:

$$\begin{cases} M_h = \left\{ u_h \in M / \forall K \in \mathcal{T}_h,\ u_h\,|_K \in (Q_0(K))^2 \right\}, \\ X_h = \left\{ \sigma_h \in X / \forall K \in \mathcal{T}_h,\ \sigma_h\,|_K \in (Q_1(K))^4 \right\}, \\ X_h^s = \left\{ \sigma_h \in X_h / \mathbf{as}(\sigma_h) = 0 \right\}, \end{cases} \tag{5.24}$$

where $Q_k(K)$ denotes the space of polynomials on K of the form $p(x_1, x_2) = \sum\limits_{0\leq i,j\leq k} c_{ij} x_1^i x_2^j$. In this case the approximation problem, associated to the mixed velocity-stress system for elastodynamics, can be written in the following form :

$$\begin{cases} \text{Find } (\sigma_h, v_h) : \mathbb{R}^+ \to X_h^s \times M_h \text{ such that :} \\ \dfrac{d}{dt} a(\sigma_h(t), \tau_h) + b(\tau_h, v_h(t)) = 0\ ,\ \forall \tau_h \in X_h^s, \\ \dfrac{d}{dt} c(v_h(t), w_h) - b(\sigma_h(t), w_h) = (f, w_h)\ ,\ \forall w_h \in M_h. \end{cases} \tag{5.25}$$

We present in Fig. 4 the degrees of freedom in the new element. In Fig. 4-right we consider a node of the mesh and we present the degrees of freedom (corresponding to the stress tensor) that are associated to this node.

Remark 6

• *One could think that the most natural choice for the construction of the space* X_h *would be the lowest order Raviart Thomas element*[23,11] $RT_{[0]}$*:*

$$\begin{aligned} X_h^{RT} &= \left\{ \sigma_h \in X / (\sigma_{h1}, \sigma_{h2}) \in (RT_{[0]})^2 \right\}, \\ RT_{[0]} &= P_{1,0} \times P_{0,1}. \end{aligned}$$

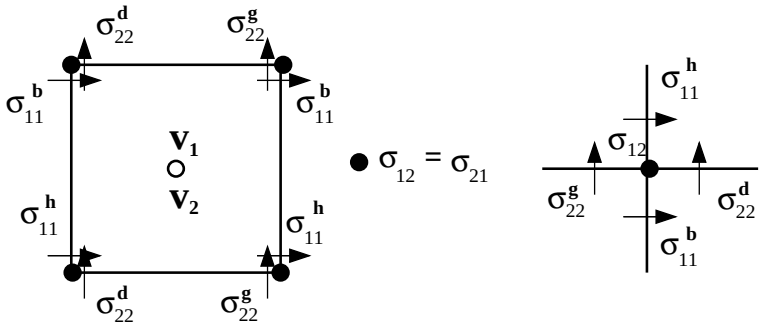

Figure 4: Degrees of freedom for the $Q_1^{\mathrm{div}} - Q_0$ element.

The difficulty is that the space $X_h^{RT} \cap X^s$ is too small and thus is not a good approximation space of X^s: if σ_h is a symmetric tensor in X_h^{RT}, then σ_{12} is necessarily constant! (σ_{12} is linear in x_2 and constant in x_1 while σ_{21} is linear in x_1 and constant in x_2).

• *Another approach, which was developed for the stationary problem, and permits to avoid this difficulty consists in imposing the symmetry of the stress tensor* $\mathbf{as}(\sigma) = 0$ *in a weak way and introducing the corresponding Lagrange multiplier. Following this approach for the transitory problem, we can show that the continuous problem (3.3) is equivalent to :*

$$\begin{cases} \text{Find } (\sigma, v, \gamma) : \mathbb{R}^+ \to X \times M \times L \text{ such that :} \\ \dfrac{d}{dt} a(\sigma(t), \tau) + b(\tau, v(t)) + d(\tau, \gamma(t)) = 0, & \forall \tau \in X^s, \\ \dfrac{d}{dt} c(v(t), w) - b(\sigma(t), w) = (f, w), & \forall w \in M, \\ d(\sigma(t), \mu) = 0, & \forall \mu \in L, \end{cases}$$

where γ corresponds to rot$(v)/2$, $L = L^2(\Omega)$ and the bilinear form $d(\cdot, \cdot)$ is defined by

$$d(\sigma, \mu) = \int_\Omega \mathbf{as}(\sigma)\ \mu\ dx, \quad \forall (\sigma, \mu) \in H \times M.$$

It is from this type of formulation, or more precisely from its equivalent for the stationary problem, that PEERS element was constructed[1]*. We did not follow this technique because it does not lead to an explicit scheme after time discretization.*

Our space X_h^s is constructed from the second family of mixed finite elements proposed by Nédélec[21]. It presents two advantages, the first one concerns the symmetry of the stress tensor which is taken into account in a strong way (the symmetry is included in the approximation space), the second one concerns obtaining an explicit time discretization scheme using mass-lumping techniques.

Strong symmetry: Using the regular structure of the mesh, it is easy to see that, if $\sigma_h \in X$ and $\sigma_h|_K \in \mathcal{P}(K)$, where $\mathcal{P}(K)$ is a set of polynomial functions on K, then σ_h

satisfies the following continuity properties: (i) σ_{11} is continuous in the x_1 direction (not necessarily in the x_2 one) and σ_{22} is continuous in x_2 , therefore the vector $(\sigma_{11}, \sigma_{22})^t$ is in $H(\text{div})$ (ii) on the other hand σ_{12} is continuous in x_2 and σ_{21} is continuous in x_1, thus relation $\sigma_{12} = \sigma_{21}$ implies that σ_{12} is continuous in Ω (namely it belongs to H^1). This remark has led us to choose for σ_{12} a Q_1 continuous function. The choice of Q_1 elements for $(\sigma_{11}, \sigma_{22})^t$ follows from our requirement of mass lumping (see below).

Mass lumping: In order to obtain an explicit time discretization scheme we need to use a mass lumping technique for the approximation of the mass matrix associated to the bilinear form $a(\sigma_h, \tau_h)$ (the reader can verify that the matrix associated to $c(u_h, v_h)$ is already diagonal in the usual basis of M_h). We first remind that the basic principle of mass-lumping consists in approximating the integrals appearing in the mass matrix using a quadrature formula of the form:

$$\int_K f dx \approx I_K(f) \equiv \sum_{i \in K} f(M_i)\omega_i,$$

where M_i are the quadrature points and ω_i the associated weights. The key point is then to find an adequate quadrature formula which will lead to a diagonal mass matrix. For instance, if we wanted to approximate the scalar acoustic wave equation with the classical Q_1 element, the integrals appearing in the mass matrix would be $\int_K w_i w_j dx$ with $w_i(M_j) = \delta_{ij}$ the Lagrange basis functions and M_j the nodes of the mesh (summits of the elements). One can easily check that the use of the following quadrature formula:

$$\int_k f dx \approx I_K(f) = \frac{h^2}{4} \sum_{M \text{ summits of } K} f(M) \qquad \forall f \in C^o(K) \tag{5.26}$$

leads now to a diagonal mass matrix. In our case, following the same principle, we are led to approximate the mass matrix $a(\sigma_h, \tau_h)$ by :

$$a_h(\sigma_h, \tau_h) = \sum_{K \in \mathcal{T}_h} I_K(A\sigma_h : \tau_h),$$

where the use of the quadrature formula (5.26) on K leads now to a block diagonal mass matrix. Each block is associated to a node of the mesh and its dimension is equal to the number of degrees of freedom at this point (that is 5, see Fig. 4-right).

Approximation properties: for M_h, one has the classical properties:

$$\begin{cases} \forall v \in M, \ \lim\limits_{h \to 0} \inf\limits_{w_h \in M_h} \|v - w_h\|_M = 0, \\ \forall v \in (H^1(\Omega))^2, \ \inf\limits_{w_h \in M_h} \|v - w_h\|_M \leq Ch \|v\|_1 . \end{cases}$$

On the other hand, one can show (see Remark below):

$$\begin{cases} \forall \sigma \in X^s,\ \lim\limits_{h\to 0} \inf\limits_{\tau_h \in X_h^s} \|\sigma - \tau_h\|_{X^s} = 0, \\ \forall \sigma \in (H^1(\mathrm{div},\Omega))^2 \cap X^s,\ \inf\limits_{\tau_h \in X_h^s} \|\sigma - \tau_h\|_{X^s} \leq Ch\, \|\sigma\|_{H^1(\mathrm{div})}\,. \end{cases} \tag{5.27}$$

Remark 7 *In a recent paper*[8]*, the scalar version of this element is presented, for the approximation of the scalar anisotropic wave equation. In particular, it is explained why the use of Raviart-Thomas elements do not allow to achieve mass-lumping while this element does. For the analysis of this element, the difficulty is that it does not enter the classical Babuska-Brezzi theory (compared to the choice* $RT_{[0]}, Q_0$ *usually used for the pressure and velocity, we have enriched the space of the pressures). That is why we have proposed a modified abstract theory which permits us to get non-classical error estimates. However, the theory developed there can not be directly applied to the elastodynamic problem, it has to be again modified, see* [7]*. In particular, approximation properties (5.27) follow from this theory.*

6. Stability and dispersion analysis of the $Q_1^{\mathrm{div}} - Q_0$ element in the case of a homogeneous, isotropic medium.

We study the lowest order mixed finite element $Q_1^{\mathrm{div}} - Q_0$ for a homogeneous, isotropic medium. In this case, the discretization scheme can be interpreted as a finite difference scheme and thus can be analyzed by the usual techniques: dispersion and stability analysis. Similar analysies have been performed for higher-order elements and in 3D[24].

6.6.1. *Interpretation as a finite difference scheme*

We will describe here the numerical scheme obtained after space discretization of problem (5.25) in a regular mesh. We can see that we have periodicity of two types of nodes (cf.

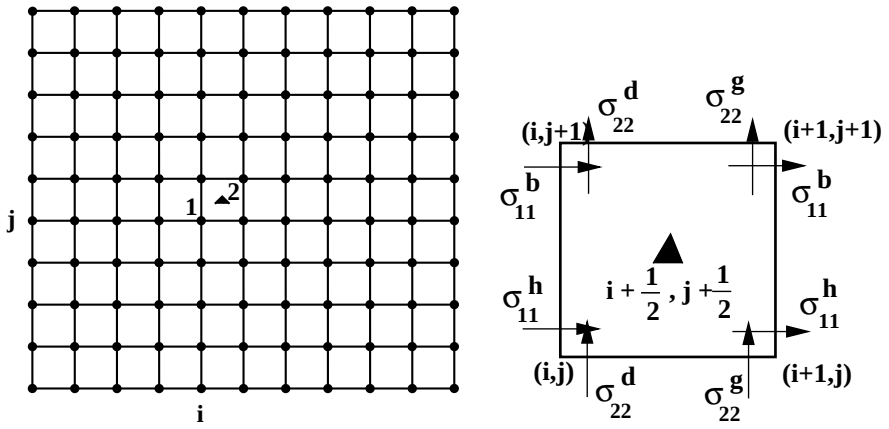

Figure 5: Left: The mesh. Right: Degrees of freedom

Fig. 5-left). The points 1 and 2 will be respectively indexed by (i, j) and $(i + 1/2, j + 1/2)$.

At each point of type 1 correspond 5 degrees of freedom, see Fig. 5-right : σ_{11}^h, σ_{11}^b, σ_{22}^d, σ_{22}^g and σ_{12}. At each point of type 2 correspond 2 degrees of freedom, the two components of the velocity: v_1 and v_2. After some calculations (we do not enter here into details), system (5.25) can be rewritten as a finite difference scheme, and the unknown σ can be eliminated. We end up with a second order scheme in time on the velocity, that can be written in matrix form:

$$\frac{d^2V}{dt^2} = \mathbb{K}_h V \quad \text{with} \quad \mathbb{K}_h = \begin{bmatrix} V_p^2\mathcal{D}_{\alpha,1}^2 + V_s^2\mathcal{D}_{\beta,2}^2 & (V_p^2 - V_s^2)D_{12} \\ (V_p^2 - V_s^2)D_{12} & V_p^2\mathcal{D}_{\alpha,2}^2 + V_s^2\mathcal{D}_{\beta,1}^2 \end{bmatrix}, \tag{6.28}$$

where $V = (v_1, v_2)^t$ and $\mathcal{D}_{\alpha,1}^2 f(i,j) = \alpha D_1^2 f(i,j-1) + (1-2\alpha)D_1^2 f(i,j) + \alpha D_1^2 f(i,j+1)$, D_1^2 being the discrete operator (classical second order, centered, finite differences operator):

$$D_1^2 f(i,j) = \frac{f(i+1,j) - 2f(i,j) + f(i-1,j)}{h^2}.$$

We can remark that (6.28) defines a general class of second order numerical schemes, depending on two parameters α and β with ($0 \le \alpha \le 1/2,\ 0 \le \beta \le 1/2$). In particular, $\alpha = 0,\ \beta = 0$ correspond to the finite differences scheme, $\alpha = 1/6,\ \beta = 1/6$ to the Q_1 finite elements scheme and $\alpha = (V_p^2 - 2V_s^2)^2/(4V_p^4)$, $\beta = 1/4$ to the $Q_1^{\text{div}} - Q_0$ mixed finite elements scheme. Note that, for the new scheme, α depends on the Poisson's coefficient $\nu = \lambda/(2(\lambda+\mu))$, which means that it is adapted to the considered elastic medium.

Remark 8 *System (6.28) is an approximation of the elastodynamic problem, written in displacement:*

$$\frac{d^2V}{dt^2} = \mathbb{K} V \quad \textit{with} \quad \mathbb{K} = \begin{bmatrix} V_p^2\dfrac{\partial^2}{\partial x_1^2} + V_s^2\dfrac{\partial^2}{\partial x_2^2} & (V_p^2 - V_s^2)\dfrac{\partial^2}{\partial x_1 \partial x_2} \\ (V_p^2 - V_s^2)\dfrac{\partial^2}{\partial x_1 \partial x_2} & V_p^2\dfrac{\partial^2}{\partial x_2^2} + V_s^2\dfrac{\partial^2}{\partial x_1^2} \end{bmatrix}. \tag{6.29}$$

6.6.2. *Stability condition*

For the time discretization of problem (6.28) we use the classical second order centered finite differences approximation and get the total discretized scheme:

$$\frac{V^{n+1} - 2V^n + V^{n-1}}{\Delta t^2} = \mathbb{K}_h V^n. \tag{6.30}$$

The stability condition for this scheme is:

$$\frac{\Delta t^2 \, \|\mathbb{K}_h\|}{4} \le 1.$$

In order to compute $\|\mathbb{K}_h\|$ we will use the Fourier transform in space :

$$\forall f(x_1,x_2) \in L^1(\mathbb{R}^2) \text{ we have : } \hat{f}(k_1,k_2) = \frac{1}{\sqrt{2\pi}} \int_{\mathbb{R}^2} f(x_1,x_2) \exp^{-i(k_1x_1 + k_2x_2)} \, dx_1 dx_2.$$

From Parseval's identity, we get

$$\|\mathbb{K}_h\| = \sup_{\vec{k}} \left\| \widehat{\mathbb{K}_h}(\vec{k}) \right\| = \max_{i=1,2} \sup_{(X_1,X_2)\in[0,1]^2} \lambda_i(X_1, X_2), \tag{6.31}$$

where $\lambda_i(X_1, X_2),\ i = 1, 2$ are the two eigenvalues of the symmetric matrix $\widehat{\mathbb{K}_h}$, whose components are expressed in terms of $X_1 = \sin^2(\frac{k_1 h}{2})$ and $X_2 = \sin^2(\frac{k_2 h}{2})$, and are:

$$\begin{cases} \widehat{\mathbb{K}_h}[1,1] = \dfrac{1}{h^2}\left(4V_p^2 X_1(1-4\alpha X_2) + 4V_s^2 X_2(1-4\beta X_1)\right), \\ \widehat{\mathbb{K}_h}[2,2] = \dfrac{1}{h^2}\left(4V_p^2 X_2(1-4\alpha X_1) + 4V_s^2 X_1(1-4\beta X_2)\right), \\ \widehat{\mathbb{K}_h}[1,2] = \dfrac{4}{h^2}\left(V_p^2 - V_s^2\right)\sqrt{X_1(1-X_2)}\sqrt{X_2(1-X_1)}. \end{cases} \tag{6.32}$$

Theorem 2 *The scheme (6.30) is stable under the CFL condition*

$$\frac{V_{CFL}\Delta t}{h} \leq 1, \quad \textit{with} \quad V_{CFL} = \frac{h}{2}(\max_{i=1,2} \max_{(X_1,X_2)\in[0,1]^2} \lambda_i(X_1, X_2))^{1/2}. \tag{6.33}$$

The value of V_{CFL} depends on parameters α and β, see Fig. 6:

- *In domain I: $V_{CFL} = \sqrt{V_p^2 + V_s^2 - 4(\alpha V_p^2 + \beta V_s^2)}$.*
- *In domain II, the value is constant: $V_{CFL} = V_p$.*

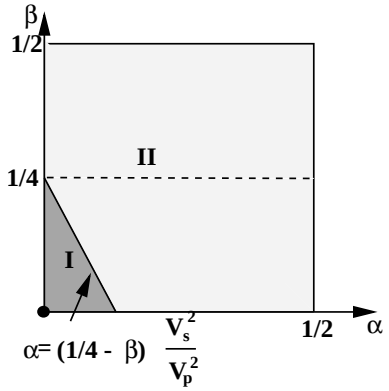

Figure 6: Stability Domains

Proof: We only indicate the main steps of the proof (for more details, see[24]).
• We first study the characteristic polynomial and show that, if the maximum of the greater eigenvalue is reached in the interior of the square, then it is on a point located on the diagonal $X_1 = X_2$. In other terms, this maximum is reached either on the diagonal $X_1 = X_2$ or on the border of the square $[0, 1]^2$.

• The expressions of the eigenvalues are the following, for $i = 1, 2$

$$\begin{aligned}\lambda_i(X_1, X_2) &= \frac{2}{h^2}\left[(V_p^2 + V_s^2)(X_1 + X_2) - 8(\alpha V_p^2 + \beta V_s^2)X_1X_2\right] \\ &\pm \frac{2}{h^2}(V_p^2 - V_s^2)\sqrt{(X_1 - X_2)^2 + 4(X_1 - X_1^2)(X_2 - X_2^2)}\end{aligned} \tag{6.34}$$

We then prove that the maximum of the greater one is necessarily reached at a vertex of the square and get the result. ■

For the finite differences scheme ($\alpha = \beta = 0$) the maximum is in domain I, $V_{CFL}^{FD} = \sqrt{V_p^2 + V_s^2}$, while for the Q_1 finite elements as well as for the $Q_1^{\text{div}} - Q_0$ mixed finite element the maximum is in domain II, $V_{CFL}^{Q_1} = V_{CFL}^{Q_1^{\text{div}} - Q_0} = V_p < V_{CFL}^{FD}$, and therefore is better than with finite differences. In the following, we will call CFL ratio the quantity $\alpha_{CFL} = \Delta t/h$ and we denote by α_{CFL}^{FD}, $\alpha_{CFL}^{Q_1} = \alpha_{CFL}^{Q_1^{\text{div}} - Q_0}$ the maximum allowed by the stability condition for each scheme (i.e., $\alpha_{CFL}^{FD} = 1/V_{CFL}^{FD} < \alpha_{CFL}^{Q_1} = 1/V_{CFL}^{Q_1}$).

6.6.3. *Dispersion Analysis for the total discretized scheme*

For the continuous problem, the dispersion analysis consists in searching plane waves solutions of system (6.29), i.e., waves of the following form:

$$U = U_o \exp \imath(k_1x_1 + k_2x_2 - \omega t), \quad U_o \in \mathbb{R}^2, \quad k = (k_1, k_2) \in \mathbb{R}^2, \quad \omega \in \mathbb{R}, \tag{6.35}$$

where k is the propagating direction and ω/k the phase velocity. To be a solution, U has to verify the so called dispersion relation :

$$\omega^2 U_o = \widehat{\mathbb{K}} U_o \quad \text{where} \quad \widehat{\mathbb{K}} = \begin{bmatrix} V_p^2 k_1^2 + V_s^2 k_2^2 & (V_p^2 - V_s^2)k_1k_2 \\ (V_p^2 - V_s^2)k_1k_2 & V_p^2 k_2^2 + V_s^2 k_1^2 \end{bmatrix}. \tag{6.36}$$

Equation (6.36) implies that ω^2 is an eigenvalue of $\widehat{\mathbb{K}}$ and U_o is the associated eigenvector. Therefore, we have[4]

$$\begin{aligned}\omega_1^2 &= V_p^2(k_1^2 + k_2^2), \quad U_o^1 = (k_1, k_2), \\ \omega_2^2 &= V_s^2(k_1^2 + k_2^2), \quad U_o^2 = (-k_2, k_1),\end{aligned} \tag{6.37}$$

where ω_1 corresponds to a Pressure wave, propagating with the phase velocity $V_p = \omega_1/|k|$ and ω_2 corresponds to a Shear wave, propagating with the phase velocity $V_s = \omega_2/|k|$. Phase velocities V_p and V_s are independent of ω, we say that the elastodynamic equation is non-dispersive. To study the dispersion relation of scheme (6.30) we search particular solutions of (6.28) in the form:

$$U_{ij} = U_{oh} \exp \imath(k_1x_1^i + k_2x_2^j - \omega t), \quad U_{oh} \in \mathbb{R}^2, \quad k = (k_1, k_2) \in \mathbb{R}^2, \quad \omega \in \mathbb{R}. \tag{6.38}$$

We can prove the existence of numerical waves P and S which are dispersive. The dispersion relation for scheme (6.30) is:

$$\frac{4}{\Delta t^2}\sin^2(\frac{\Delta t\omega_h}{2})\ U_{oh} = \widehat{\mathbb{K}_h}U_{oh},$$

where $\widehat{\mathbb{K}_h}$ is the symmetric matrix defined by (6.32). We then obtain for $i = 1, 2$

$$\frac{4}{\Delta t^2}\sin^2(\frac{\Delta t\omega_h^i}{2}) = \lambda_i(X_1, X_2), \quad (\lambda_i \text{ defined in (6.34)}). \tag{6.39}$$

We set $k = (k_1, k_2)$, where the components of k are related to the angle of propagation ϕ by $k_1 = |k|\cos\phi, \quad k_2 = |k|\sin\phi$. Let $V_h = \dfrac{\omega_h}{|k|}$ be the numerical phase velocity. We introduce the adimensional quantity q_p (resp. q_s) which represents the ratio between the numerical and the continuous phase velocity of the P (resp. S) waves :

$$q_p = \frac{\omega_h^1}{|k|\,V_p}\ ;\ q_s = \frac{\omega_h^2}{|k|\,V_s} \tag{6.40}$$

If we set $K = \dfrac{1}{N} = \dfrac{|k|\,h}{2\pi}$, with N the number of points per wavelength, we notice that q_p (resp. q_s) depends on the discretization parameter K, on the angle of propagation ϕ, on the Poisson's coefficient $\nu = \dfrac{\lambda}{2(\lambda+\mu)}$ and on the step size Δt (or equivalently on the CFL ratio α_{CFL}). We compare the dispersion of the $Q_1^{\text{div}} - Q_0$ mixed finite element scheme (red), the dispersion of the classical Q_1 finite element scheme (blue) and the dispersion of the classical finite difference scheme (green). For each scheme, we plot q_p and q_s with respect to K, and this for several values of the Poisson's coefficient, for several angles and for the maximum value of the CFL ratio α_{CFL} allowed by the stability condition. Actually, we can check that the dispersion error for P waves decreases as α_{CFL} increases, we have thus chosen to represent the best curves for the dispersion of P waves. We present in Fig. 9 the curves obtained for $\nu = 0.1$, and for the angles $\phi = 0, 15, 30$ and 45 degrees, but the observations we do here are the same for other values of ν. Concerning P waves: the $Q_1^{\text{div}} - Q_0$ and Q_1 elements have their worse dispersion for the diagonal direction $\phi = 45$ and become better when the direction becomes parallel to the grid axis $\phi = 0$, and it is the contrary for the FD scheme. For S waves, the $Q_1^{\text{div}} - Q_0$ and Q_1 elements have again a monotone behavior with respect to the angle, which is inverted compared to P waves, i.e., they have their worse dispersion for $\phi = 0$ and become better for $\phi = 45$. On the other hand, one cannot conclude for the FD scheme, since the results change depending on the angle ϕ and on the value of ν.

We represent in Fig. 10 the "worse" curves for each scheme, for two values of ν. We can see that, in all cases, the new finite element $Q_1^{\text{div}} - Q_0$ is always better than (or identical to) the Q_1 element (with the same CFL ratio). The comparison with FD is not so clear for P waves: if we fix the number of points per wavelength, the FD can become in some cases better than the $Q_1^{\text{div}} - Q_0$ (e.g., $\nu = 0.4$, P waves) but with a smaller CFL ratio, i.e., it is

also more expensive. On the other hand, the $Q_1^{\rm div} - Q_0$ always gives a better (or identical) dispersion than FD for S waves, which are slower than P waves ($V_s < V_p$) and thus more difficult to approximate.

In conclusion, if we consider both stability and dispersion, our scheme has a better behavior than Finite Differences and than Q_1. This was not a priori expected since this element was designed for different purposes (strong symmetry and mass lumping).

7. Numerical Results

We will present in this section three numerical experiments. In the first two examples, without topography, we want to validate the lowest order new mixed finite element and the absorbing layers in isotropic and anisotropic media. The last example shows the efficiency of the coupling with the fictitious domain method in a heterogeneous medium. For the time discretization we use the classical centered finite difference scheme of 2nd order. In each case, we solve the elastodynamic problem with zero initial conditions, and with an explosive source located at point $S = (x_1^s, x_2^s)$,

$$f(x_1, x_2, t) = F(t)g(r),$$

where

$$\left\{ \begin{array}{l} F(t) = \left\{ \begin{array}{ll} -2\pi^2 f_0^2 (t-t_0) e^{-\pi^2 f_0^2 (t-t_0)^2} & \text{if } t \le 2t_0 \\ 0 & \text{if } t > 2t_0 \end{array} \right. , \\ t_0 = \dfrac{1}{f_0}, \quad f_0 = \dfrac{V_s}{h}\dfrac{1}{N_S} \text{ is the central frequency,} \\ N_S \text{ is the number of points per S wave length,} \end{array} \right. \tag{7.41}$$

and $\vec{g}(r)$ is a radial function :

$$\left\{ \begin{array}{l} \vec{g}(r) = \left(1 - \dfrac{r^2}{a^2}\right)^3 \; 1_{B_a} \; \vec{e}, \\ r = \sqrt{(x_1 - x_1^s)^2 + (x_2 - x_2^s)^2}, \; a = 5h \; , \end{array} \right. \tag{7.42}$$

where 1_{B_a} is one on B_a, the disk of center S and radius a, and zero elsewhere and $\vec{e}$ will be precised in each experiment. The absorbing layer model is characterized by the length δ of the layer, and the damping parameter (see Fig. 7-right)

$$d(x_1) = d_0 \left(\frac{x_1}{\delta}\right)^2, \quad \text{with} \;\; d_0 = \left|\log\left(\frac{1}{R}\right)\right| \frac{3V_p}{2\delta}, \tag{7.43}$$

and R is the reflection coefficient predicted by the theory [13], δ and R being defined in each case. The domain C is meshed with $N \times N$ squares of edge h. The time step is computed following the CFL condition $\Delta t = h/V_p$.

Remark 9 *In a heterogeneous medium, we choose*

$$f_0 = \frac{\min V_s}{h}\frac{1}{N_S}, \quad d_0 = \left|\log\left(\frac{1}{R}\right)\right| \frac{3 \max V_p}{2\delta}, \quad \textit{and} \;\; \Delta t = \frac{h}{\max V_p},$$

where the max *and the* min *are the extremal values of the velocities on the whole domain.*

7.7.1. *Rayleigh waves and PML*

In the first example we consider the elastic wave propagation problem in the homogeneous isotropic half plane ($x_2 < 0$) where the source point S is near the free surface. We have chosen this problem in order to test the efficiency of the PML model on the Rayleigh wave, which is particularly difficult to absorb. In order to approximate this problem we consider a bounded domain $C = [0, 100] \times [-100, 0]$ with absorbing layers (PML) on the artificial boundary Γ_A (see Fig. 7-left). The velocities in the medium are $V_p = \sqrt{5}$, $V_s = \sqrt{2}$. The

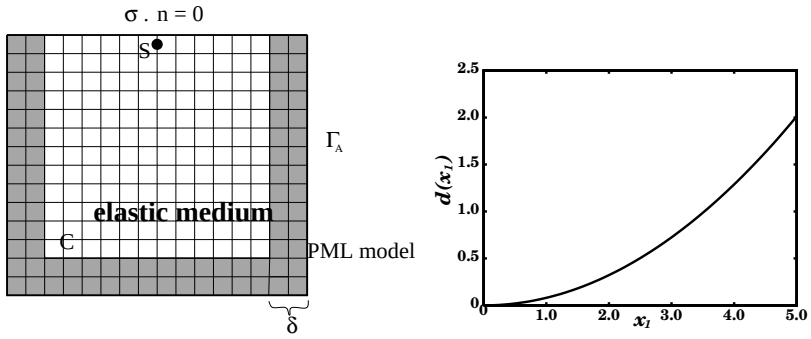

Figure 7: Left: The bounded domain problem. Right: The damping coefficient $d(x)$

uniform grid on C is composed of squares of edge $h = 0.5$. To complete the characteristics of the source, given in (7.41) and (7.42), we choose $\vec{e} = (\frac{x_1 - x_1^s}{r}, \frac{x_2 - x_2^s}{r})$ and the point source $S = (50, 97)$. The length of the absorbing layer is $\delta = 10h$ and the theoretical reflection coefficient is $R = 0.001$. In Fig. 11, we represent the solution of this problem at different times. We can see two cylindrical waves propagating with two different velocities (Pressure wave and Shear wave) and we can also observe the Rayleigh wave propagating along the surface with a velocity roughly equal to the velocity of shear waves. We can remark that PML model absorbs efficiently the cylindrical waves P, S and the Rayleigh wave. More precisely the reflection coefficient is in this case $R = 0.001$: this is the value predicted by the theory, and looking carefully on the figures (change of scale), we can check that this is also approximately the numerical value.

7.7.2. *Homogeneous, anisotropic elastic medium.*

We consider here a homogeneous, anisotropic, elastic medium: the apatite. Again the computational domain is a square C surrounded by absorbing layers on all four boundaries. The characteristics of the problem are: $N = 240$, $h = 0.33m$, $N_S = 10$. We use a x_2-directional point load source, $\vec{e} = (0, 1)$. The source is located at the center of the frame $S = (40m, 40m)$. The length of the absorbing layers is $\delta = 5h$ and the reflection coefficient $R = 0.01$. The material is characterized by its density and the matrix of elastic coefficients:

$$C = \begin{pmatrix} 16.7 & 6.6 & 0. \\ 6.6 & 14. & 0. \\ 0 & 0 & 6.63 \end{pmatrix} 10^{11} Pa \quad ; \quad \rho = 3.2 gr/cm^3$$

In a 2D anisotropic medium, there are two waves propagating, the Quasi-Pressure wave (QP) and the Quasi-Shear wave (QS). Before giving the numerical results, we present in Fig. 12 the theoretical wave fronts curves for the Apatite and the amplitudes of the QP and QS waves for a x_2-directional point load source. In Fig. 13, we represent the solution of this problem at different times. We can remark that the wave front curves and the amplitude of the Quasi-Pressure and the Quasi-Shear wave computed numerically show the characteristics predicted theoretically : the Quasi-Pressure wave is weaker than the Quasi-Shear wave, the amplitude of the Quasi-Pressure wave is weaker in the x_1-direction while the amplitude of the Quasi-Shear wave is weaker in the x_2-direction.

7.7.3. *Coupling with the fictitious domain method: the case of a heterogeneous elastic medium with complex topography*

We consider now the elastic wave propagation problem in a heterogeneous, isotropic medium with complex topography. To approximate this problem we consider a bounded domain $C = [0, 80] \times [0, 80]$ with absorbing layers (PML) on the artificial boundary Γ_A (see Fig. 8). As we can see in Fig. 8 the mesh on the domain C is independent of the mesh on Γ_S. The heterogeneous elastic medium considered here is characterized by the velocity

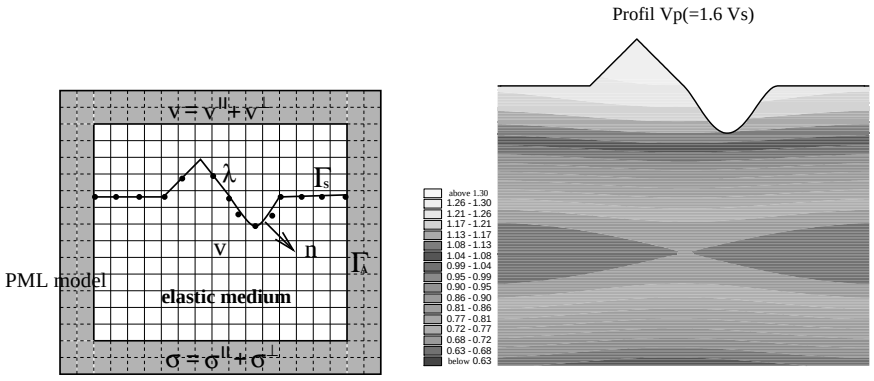

Figure 8: Left: The two meshes. Right: The velocity model for the heterogeneous medium, $\max V_p / \min V_p = 2.1$ and $V_p = 1.6 V_s$.

model presented on Fig. 8-right, we have $\max V_p / \min V_p = 2.1$ and $V_p = 1.6 V_s$. For the discretization we take V_p and V_s piecewise constants (one value per element). The step of the uniform grid on C is $h = 1/3$, and the number of points per S wavelength (for the minimum S velocity, see Remark 9) is $N_S = 10$. The source is determined by $\vec{e} = (\dfrac{x_1 - x_1^s}{r}, \dfrac{x_2 - x_2^s}{r})$ and the point source is located at $S = (36.67, 56.67)$. On the free surface Γ_S we use an 1D irregular mesh. The length of the absorbing layer is $\delta = 10h$ and the damping parameter is chosen according to (7.43) and Remark 9 with a reflection coefficient $R = 0.01$. In Fig. 14, we represent the norm of the velocity at different times. We can observe that the wave fronts are not circular, because of the heterogeneities, and the energy is localized in some

regions. Although the phenomena are more complicated than in a homogeneous medium, one can see P and S waves reflected by the topography (the P wave being faster than the S one), and one can also see a diffraction by the wedge. There is a surface wave propagating along the topography, which is again very well absorbed by the PMLs.

8. Conclusion

We have presented a new method for solving the elastodynamic problem in anisotropic, heterogeneous media, with topographies of complex geometries. The numerical results, obtained with the lowest order element, show its efficiency in several situations. Let us mention that this method can also be applied in media containing cracks (see[9]). The new elements can be extended in a natural way to higher orders[24] and to 3D. A forthcoming paper is in preparation for the 3D case, where we treat, in particular, the additional difficulties linked to the interaction between the boundary mesh and the volume mesh, which involves much more geometry than in 2D.

Acknowledgments
This research was supported by a research contract between EDF/DER and INRIA. This was also a contribution to the Seismic Inversion, Geophysical Modeling and Applications Consortium Project.

1. N. Arnold, F. Brezzi, and J. Douglas. PEERS: A new mixed finite element for plane elasticity. *Japan J. Appl. Math.*, 1:347–367, 1984.
2. C. Atamian and P. Joly. Une analyse de la méthode des domaines fictifs pour le problème de Helmholtz extérieur. Technical Report 1378, INRIA, 1991.
3. B. A. Auld. *Acoustic Fields and Elastic Waves in Solids*, volume I et II. Wiley, 1973.
4. A. Bamberger, G. Chavent, and P. Lailly. Étude de schémas numériques pour les équations de l' élastodynamique linéaire. Technical report, INRIA, 1980. n^o 41.
5. E. Bécache and T. Ha Duong. A Space-Time Variational Formulation for the Boundary Integral Equation in a 2D Elastic Crack Problem. *RAIRO, M2AN*, 28,n^{o}2:141–176, 94.
6. E. Bécache, P. Joly, and C. Tsogka. Eléments finis mixtes et condensation de masse en élastodynamique linéaire. (i) construction. *C.R. Acad. Sci. Paris*, t. 325, Série I:545–550, 1997.
7. E. Bécache, P. Joly, and C. Tsogka. Mixed finite elements, strong symmetry and mass lumping for elastic waves. Technical Report 3717, INRIA, 1999. submitted in SIAM J. Num. An.
8. E. Bécache, P. Joly, and C. Tsogka. An analysis of new mixed finite elements for the approximation of wave propagation problems. *SINUM*, 37(4):1053–1084, 2000.
9. E. Bécache, P. Joly, and C. Tsogka. Some numerical experiments - applications of the fictitious domain method to elastodynamic waves. *http://www-rocq.inria.fr/˜becache/numer.html*, 99.
10. J.P. Bérenger. A perfectly matched layer for the absorption of electromagnetic waves. *Journal of Comp. Physics.*, **114**:185–200, 1994.
11. F. Brezzi and M. Fortin. *Mixed and Hybrid Finite Element Methods*. Springen–Verlag, 1991.
12. F. Collino, P. Joly, and F. Millot. Fictitious domain method for unsteady problems: Application to electromagnetic scattering. Technical Report 2963, INRIA, 1996.
13. F. Collino and C. Tsogka. Application of the PML Absorbing Layer Model to the Linear Elastodynamic Problem in Anisotropic Heteregeneous Media. Rapport de Recherche 3471, INRIA., 1998. to appear in Geophysics.
14. M.A. Dablain. The application of high order differencing for the scalar wave equation. *Geophysics*, 1(51):54–66, 1986.
15. S. Garcès. *Application des méthodes de domaines fictifs à la modélisation des structures rayonnantes tridimensionnelles*. PhD thesis, ENSAE, 1998.
16. V. Girault and R. Glowinski. Error analysis of a fictitious domain method applied to a Dirichlet problem. *Japan J. Indust. Appl. Math.*, 12(3):487–514, 1995.

17. R. Glowinski, T.W. Pan, and J. Periaux. A fictitious domain method for Dirichlet problem and applications. *Comp. Meth. in Appl. Mech. and Eng.*, pages 283–303, 1994.
18. R. Glowinski, T.W. Pan, and J. Periaux. A fictitious domain method for external incompressible viscous flow modeled by Navier-Stokes equations. *Comp. Meth. in Appl. Mech. and Eng.*, pages 283–303, 1994.
19. P. Grisvard. *Singularities in boundary value problems*. Masson, 1992.
20. M. E. Morley. A family of mixed finite elements for linear elasticity. *Numer. Math.*, 55:633–666, 1989.
21. J.C. Nédélec. A new family of mixed finite elements in $\mathbb{R}^3$. *Numer. Math.*, 50:57–81, 1986.
22. R. Stenberg. A family of mixed finite elements for the elasticity problem. *Numer. Math.*, 53:513–538, 1988.
23. P.A. Raviart and J.M. Thomas. A mixed finite element method for 2nd order elliptic problems. In *Lecture Notes in Mathematics*, number 606, pages 292–315. Proc. of math. aspects on the finite element method, Berlin Heidelberg New York: Springer, 1977.
24. C. Tsogka. *Méthodes de haute précision pour la résolution de l'équation de l'élastodynamique en 3D dans des milieux hétérogènes comportant des fissures*. PhD thesis, University Paris IX, 1999. to appear.

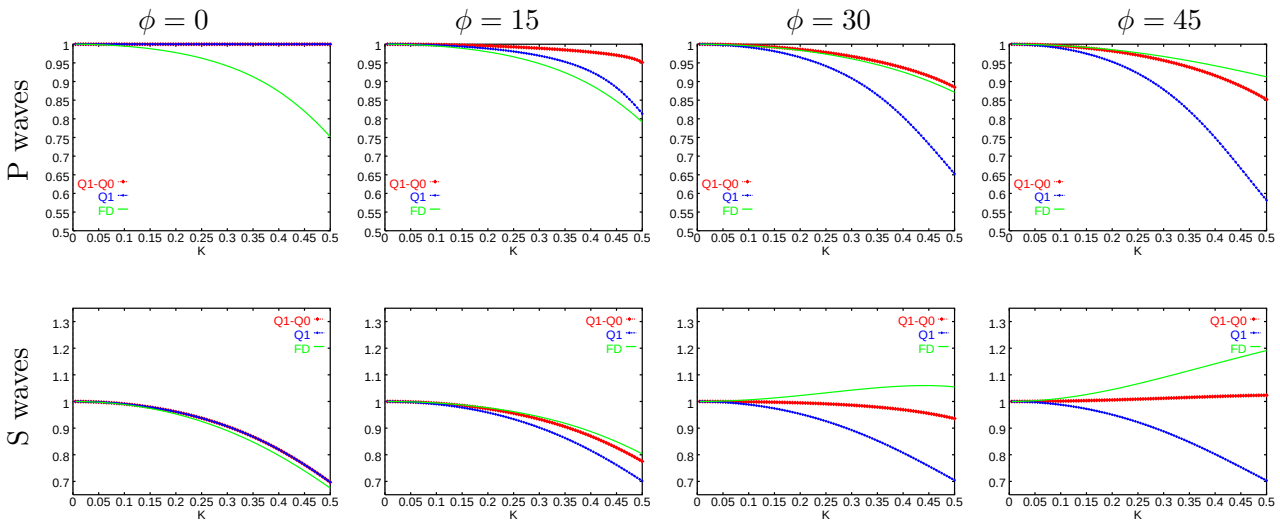

Figure 9: Phase velocity, $\nu = 0.1$.

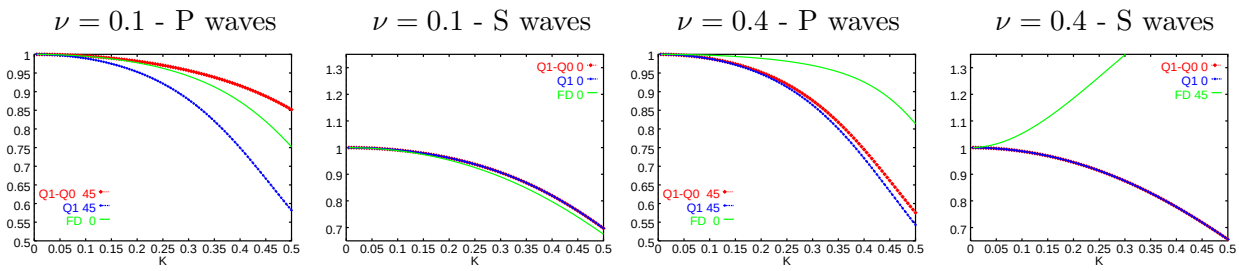

Figure 10: Comparison between the worse curves for $\nu = 0.1$ and $\nu = 0.4$

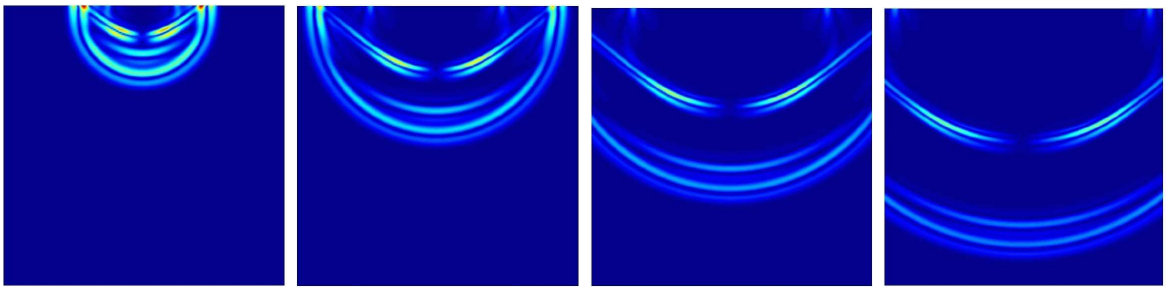

Figure 11: $|\vec{v}| = \sqrt{v_1^2 + v_2^2}$ at times between $t = 13.44$s (left) and $t = 26.88$s (right).

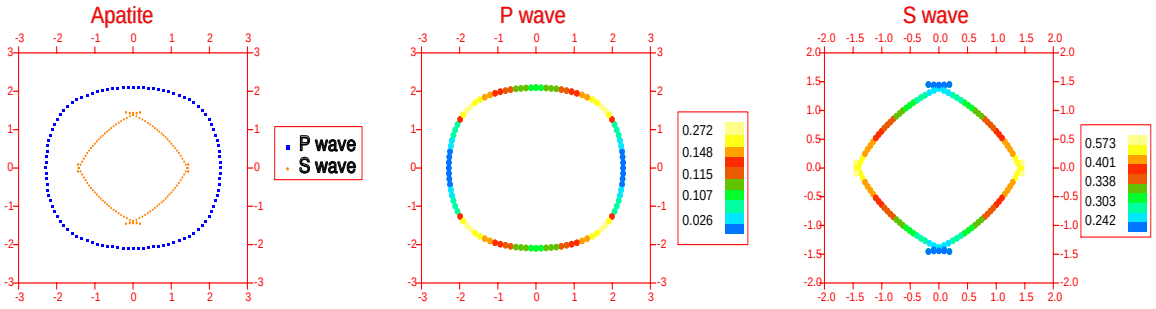

Figure 12: Left: Wave front curves for the apatite. Right: amplitude of the P wave (left) and S wave (right)

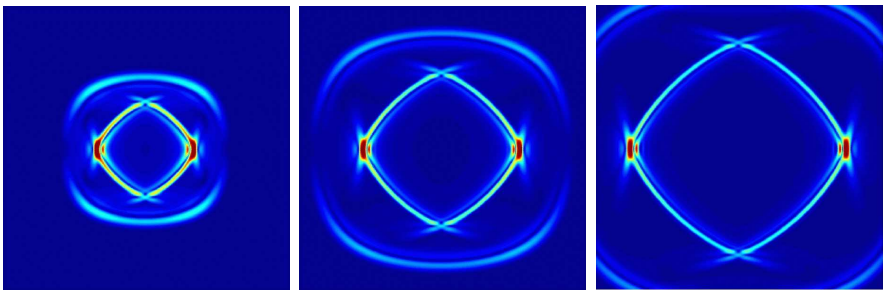

Figure 13: $|\vec{v}| = \sqrt{v_1^2 + v_2^2}$ at $t = 11.67\ s$, $17.51\ s$ and $23.35\ s$

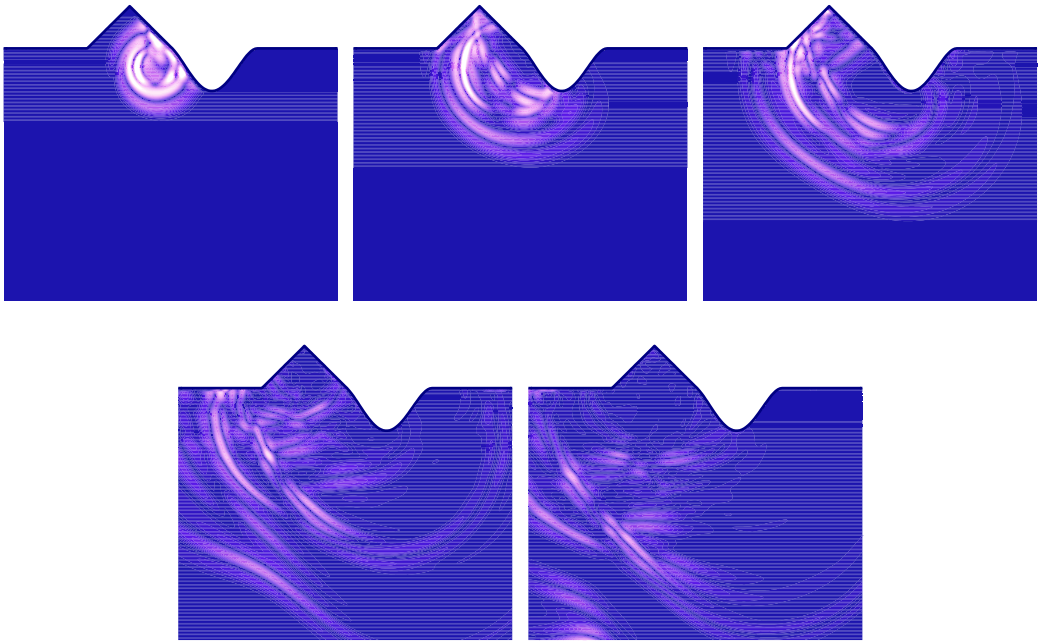

Figure 14: $|\vec{v}| = \sqrt{v_1^2 + v_2^2}$ at $t = 19.35\ s,\ 32.25\ s, 45.15\ s, 70.95\ s$ and $96.75\ s$